
# Large inverse and normal magnetocaloric effects in HoBi compound with nonhysteretic first-order phase transition

Yan Zhang(张艳), You-Guo Shi(石友国), Li-Chen Wang(王利晨), Xin-Qi Zheng(郑新奇), Jun Liu(刘俊), Ya-Xu Jin(金亚旭), Ke-Wei Zhang(张克维), Hong-Xia Liu(刘虹霞), Shuo-Tong Zong(宗朔通), Zhi-Gang Sun(孙志刚), Ji-Fan Hu(胡季帆), Tong-Yun Tong(赵同云), and Bao-Gen Shen(沈保根)

**Citation:**Chin. Phys. B, 2022, 31 (**7**): 077501. DOI: 10.1088/1674-1056/ac597f
Journal homepage: http://cpb.iphy.ac.cn; http://iopscience.iop.org/cpb

**What follows is a list of articles you may be interested in**

---

## Magnetic and magnetocaloric effect in a stuffed honeycomb polycrystalline antiferromagnet $GdInO_3$

Yao-Dong Wu(吴耀东), Wei-Wei Duan(段薇薇), Qiu-Yue Li(李秋月), Yong-Liang Qin(秦永亮),Zhen-Fa Zi(訾振发), and Jin Tang(汤进)
Chin. Phys. B, 2022, 31 (**6**): 067501. DOI: 10.1088/1674-1056/ac43a1

## Magnetism and giant magnetocaloric effect in rare-earth-based compounds $R_3BWO_9$ ($R$ = Gd, Dy, Ho)

Lu-Ling Li(李炉领), Xiao-Yu Yue(岳小宇), Wen-Jing Zhang(张文静), Hu Bao(鲍虎), Dan-Dan Wu(吴丹丹), Hui Liang(梁慧), Yi-Yan Wang(王义炎), Yan Sun(孙燕), Qiu-Ju Li(李秋菊), and Xue-Feng Sun(孙学峰)
Chin. Phys. B, 2021, 30 (**7**): 077501. DOI: 10.1088/1674-1056/abf916

## Metamagnetic transition and reversible magnetocaloric effect in antiferromagnetic DyNiGa compound

Yan-Hong Ding(丁燕红), Fan-Zhen Meng(孟凡振), Li-Chen Wang(王利晨), Ruo-Shui Liu(刘若水), Jun Shen(沈俊)
Chin. Phys. B, 2020, 29 (**7**): 077501. DOI: 10.1088/1674-1056/ab90f3

## Multicaloric and coupled-caloric effects

Jia-Zheng Hao(郝嘉政), Feng-Xia Hu(胡凤霞), Zi-Bing Yu(尉紫冰), Fei-Ran Shen(沈斐然), Hou-Bo Zhou(周厚博), Yi-Hong Gao(高怡红), Kai-Ming Qiao(乔凯明), Jia Li(李佳), Cheng Zhang(张丞), Wen-Hui Liang(梁文会), Jing Wang(王晶), Jun He(何峻), Ji-Rong Sun(孙继荣), Bao-Gen Shen(沈保根)
Chin. Phys. B, 2020, 29 (**4**): 047504. DOI: 10.1088/1674-1056/ab7da7

## Magnetocaloric effect and critical behavior of the Mn-rich itinerant material $Mn_3GaC$ with enhanced ferromagnetic interaction

Pengfei Liu(刘鹏飞), Jie Peng(彭杰), Mianqi Xue(薛面起), Bosen Wang(王铂森)
Chin. Phys. B, 2020, 29 (**4**): 047503. DOI: 10.1088/1674-1056/ab7da1

---

# Large inverse and normal magnetocaloric effects in HoBi compound with nonhysteretic first-order phase transition

Yan Zhang(张艳)[1,3], You-Guo Shi(石友国)[2], Li-Chen Wang(王利晨)[2], Xin-Qi Zheng(郑新奇)[4], Jun Liu(刘俊)[2], Ya-Xu Jin(金亚旭)[1,3], Ke-Wei Zhang(张克维)[1,3], Hong-Xia Liu(刘虹霞)[1,3], Shuo-Tong Zong(宗朔通)[1,3,†], Zhi-Gang Sun(孙志刚)[1,3], Ji-Fan Hu(胡季帆)[1,3], Tong-Yun Tong(赵同云)[2], and Bao-Gen Shen(沈保根)[2]

[1] *School of Materials Science and Engineering, Taiyuan University of Science and Technology, Taiyuan* 030024, *China*
[2] *Institute of Physics, Chinese Academy of Sciences, Beijing* 100190, *China*
[3] *Laboratory of Magnetic and Electric Functional Materials and Applications, The Key Laboratory of Shanxi Province, Taiyuan* 030024, *China*
[4] *School of Materials Science and Engineering, University of Science and Technology Beijing, Beijing* 100083, *China*

(Received 23 January 2022; revised manuscript received 25 February 2022; accepted manuscript online 2 March 2022)

HoBi single crystal and polycrystalline compounds with NaCl-type structure are successfully obtained, and their magnetic and magnetocaloric properties are studied in detail. With temperature increasing, HoBi compound undergoes two magnetic transitions at 3.7 K and 6 K, respectively. The transition temperature at 6 K is recognized as an antiferromagnetic-to-paramagnetic (AFM–PM) transition, which belongs to the first-order magnetic phase transition (FOMT). It is interesting that the HoBi compound with FOMT exhibits good thermal and magnetic reversibility. Furthermore, a large inverse and normal magnetocaloric effect (MCE) is found in HoBi single crystal in the $H$||[100] direction, and the positive $\Delta S_{\rm M}$ peak reaches 13.1 J/kg·K under a low field change of 2 T and the negative $\Delta S_{\rm M}$ peak arrives at −18 J/kg·K under a field change of 5 T. These excellent properties are expected to be applied to some magnetic refrigerators with special designs and functions.

**Keywords:** magnetocaloric effect, antiferromagnetic, rare-earth compounds

**PACS:** 75.30.Sg, 75.50.Ee, 75.50.Cc **DOI:** 10.1088/1674-1056/ac597f

## 1. Introduction

Magnetic refrigeration technology based on the magnetocaloric effect (MCE) has proven to be an alternative to traditional gas cycle refrigeration. In recent years, this technology has shifted from basic research to application development. Magnetic refrigeration technology can be used not only in domestic and industrial refrigeration fields that are closely related to human production and life, but also in many high-precision fields, such as space science, medical treatment, and low-temperature gas energy-efficient liquefaction.[1–3]

According to the positive or negative value of the magnetic entropy change, the magnetocaloric effect is divided into normal MCE ($\Delta S_{\rm M} < 0$) and inverse MCE ($\Delta S_{\rm M} > 0$). In general, the normal MCE occurs in magnetic materials with the second-order phase transitions, for example, many ferromagnetic (FM)-to-paramagnetic (PM) second-order phase transition materials were reported to exhibit large normal MCEs.[4–8] On the contrary, some materials with the first-order magnetic transitions (FOMTs) such as martensitic transition in Heusler alloys[9,10] and antiferromagnetic (AFM)–FM transition in rare earth-transition metal compounds,[11–13] were found to present the inverse MCEs. Generally speaking,achieving the temperature change of magnetic material usually requires applying or withdrawing an external magnetic field adiabatically. For common MCE materials, thermal phenomena can be observed only through this process. Recently, Liu *et al.* proposed that the properties of successive inverse and normal MCEs can be used to make a thermostat.[11] Furthermore, the inverse MCE can be used to realize adiabatic magnetization, rather than adiabatic demagnetization, during the cooling cycle.[14] This will greatly facilitate the improvement of work efficiency. At the same time, it can also be used in a reverse refrigeration cycle, which seems to be useful in multi-stage refrigeration. In summary, the inverse MCE has a potentially important role in studying and developing the magnetic refrigeration technology. However, most of the inverse MCE materials reported so far, especially low-temperature magnetic refrigeration materials, exhibit small entropy changes,[15] and the vast majority of FOMT materials are accompanied by thermal hysteresis, which will cause a certain loss of energy consumption. Therefore, it is of great significance to find a class of material with large successive inverse and normal MCEs without hysteresis.

In this work, successive inverse and normal MCEs in HoBi compound with nonhysteretic first-order phase transition are reported. The experimental details of preparing high-quality HoBi single crystals and polycrystals are also described.

[†]Corresponding author. E-mail: zongshuotong@tyust.edu.cn

## 2. Experimental details

It is difficult to obtain high-purity HoBi polycrystalline compounds by arc melting because of the volatile metal Bi at high temperatures, so the sintering method was doped in the preparation of polycrystalline samples in this work. The high-purity metals Ho and Bi with an atomic ratio of 1:1 was uniformly placed in a cylindrical alumina crucible, and then the crucible was sealed in an argon-filled quartz tube. After keeping the quartz tube at 800 °C for 5 days, the HoBi polycrystalline samples were obtained.

In our experimental preparation, high-quality HoBi single crystals were obtained by the Bi flux method. The first step was to do the preparatory work: the high-purity elements Ho and Bi with an atomic ratio of 1:10 were evenly placed into a cylindrical alumina crucible covered with quartz wool, and then the alumina crucible was sealed in a vacuum quartz tube. The next step was to implement the heat treatment process for single crystal growth: the sealed quartz tube was heated from room temperature to 950 °C, held for 5 h, and then slowly cooled to 400 °C at a rate of 4 K/h. Finally, the sample were separated from the Bi liquid centrifugally. In this way we obtained crystals with sizes between 3 mm and 5 mm.

Powder x-ray diffraction (XRD) using Cu $K\alpha$ radiation was employed to identify the crystal structure. Magnetizations were carried out on a commercial SQUID VSM magnetometer (Quantum Design).

## 3. Results and discussion

The powder XRD data of polycrystalline samples measured at room temperature are analyzed by the Rietveld refinement method, almost all the diffraction peaks can be indexed to a cubic NaCl-type structure (space group *Fm-3m*; No. 225, $Z = 4$) as shown in Fig. 1(b). The standard error $R_p$ and $R_{wp}$ are 2.1% and 2.8%, respectively. The lattice parameters of polycrystalline are determined to be $a = b = c = 6.234$ Å. Only two diffraction peaks along the (100) plane of the single crystals are displayed in Fig. 1(b) in the case of extinction. The inset of Fig. 1(b) shows the optical image of single crystal sample of HoBi. The side length of each small square in the inset is 1 mm. The inset of Fig. 1(a) displays that green spheres and relatively small orange spheres represent the Ho and Bi ions of the crystal structure. The lattice parameters of polycrystalline (single crystals) are determined to be $a = b = c = 6.234$ Å (6.228 Å). Owing to the grain size and measurement factors, the lattice parameters of polycrystalline and single crystal are slightly different from each other.

The temperature dependence of magnetization in the zero-field-cooled (ZFC) mode and in the field-cooled (FC) mode for HoBi polycrystalline compounds are measured under the field of 0.01 T as shown in Fig. 2. With temperature increasing, the HoBi compound undergoes two magnetic transitions at 3.7 K and 6 K, respectively. The peak position at 6 K has been recognized as an ordinary antiferromagnetic-to-paramagnetic (AFM–PM) transition.[16,17] Generally speaking, the metamagnetic transition from AFM ground state to FM state belongs to the first-order transition. However, the ZFC curve and the FC curve are in good consistence with each other, suggesting an excellent thermal reversibility. As is well known, the first-order phase transition is accompanied by thermal hysteresis. Recently, a non-hysteretic first-order phase transition was found in $Eu_2In$ compound.[18] It leads an interesting fundamental question to be raised, that is, whether a magnetoelastic FOMT occurs in HoBi without changing the symmetry. We will use the experimental results of first-principles and variable temperature XRD to explain the hysteresis-free phenomenon of HoBi in the future. The peak position at 6 K has been recognized as an ordinary antiferromagnetic-to-paramagnetic (AFM–PM) transition. In addition, another transition temperature at $T_t = 3.7$ K can be an antiferromagnetic-to-antiferromagnetic (AFM–AFM) transition. Of course, there will be field-induced metamagnetic (MM) transitions with the magnetic field increasing.[16,17]

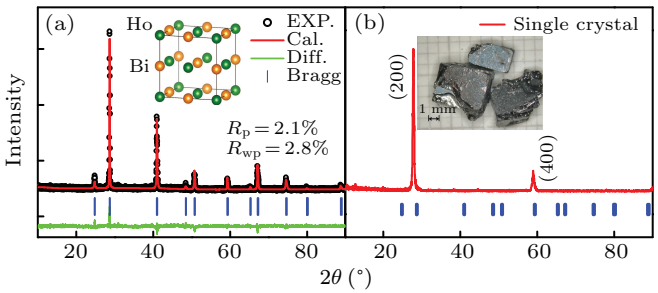


**Fig. 1.** (a) Rietveld-refined powder XRD pattern of HoBi compound at room temperature, with hollow circles representing the experiment data, continuous red line: the calculated profile, lower green curve: the difference between the measured and calculated intensity, short vertical lines: the Bragg peak positions of cubic NaCl-type structure, and inset: the crystal structure of HoBi compound. (b) XRD pattern along (200) plane of HoBi single crystal, with inset showing the optical images of single crystal sample of HoBi and side length of each small square being 1 mm.

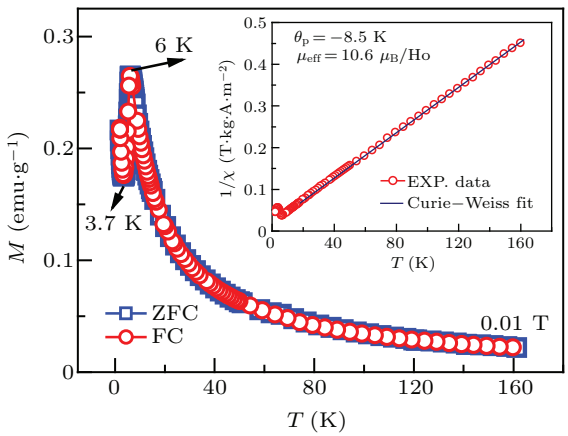


**Fig. 2.** ZFC and FC temperature dependence of magnetizations for HoBi compound under 0.01 T, where inset displays the $\chi^{-1}$–$T$ curves transformed from the measured FC curves. The solid line reaching inverse susceptibility shows the Curie–Weiss fit under 0.01 T.

The inverse susceptibility $1/\chi$ as a function of temperature under 0.01 T is plotted in the inset of Fig. 2. The effective magnetic moment is estimated at 10.6 $\mu_B$ by fitting the inversed susceptibility versus temperature curve to the Curie–Weiss law at temperature above 20 K. The fitted value is the same as the free $Ho^{3+}$ ion value (10.6 $\mu_B$), indicating that the magnetic behavior of HoBi stems from the Ho ions. Fitting to the Curie–Weiss law gives $\theta_p = -8.9$ K. This negative value is usually due to AFM coupling.

Figure 3 exhibits the magnetic hysteresis loops at 2 K of HoBi single crystal and polycrystalline. The magnetic hysteresis loop of $H \parallel [100]$ direction is measured in a field range from −7 T to 7 T. Three field-induced metamagnetic (MM) transitions on the MH curve are revealed at 1.7 T, 2.3 T, and 3.0 T, respectively, which are consistent with those reported previously.[16] The magnetization reaches saturation at 4.1-T field, and the saturation magnetic moment value is 150 emu/g. The saturation magnetic moment per Ho atom is calculated to be 10.1 $\mu_B$, which is close to the expected value of the free $Ho^{3+}$ ion (saturated moment 10.6 $\mu_B$). However, the magnetization of HoBi polycrystalline at 2 K is still increasing even at 5 T as shown in the insert of Fig. 3. This may result from the crystalline field effect, which leads to the anisotropy of HoBi. The critical field of metamagnetic transition determined by the maximum value of $\partial M/\partial H$ is 1.3 T, which is lower than the first metamagnetic transition (1.7 T) of HoBi single crystal with the magnetic field parallel to the [100] axis. It indicates that the [100] axis is difficult to magnetize due to a strong antiferromagnetic coupling effect. The magnetic structure and magnetization curves below $T_N$ with $H[110]$ have been reported in Ref. [17]. It is found that the first magnetic transition in the [110] direction occurs at about 1.3 T, and the magnetization reaches saturation with the magnetic field increasing to 2.5 T.[17] Since the local f-moments on Ho atoms are parallel within each [111] plane and antiparallel between alternating planes, the magnetization is easier to implement in the [110] direction under low magnetic field. To better understand the array of magnetic moments, a magnetic structure diagram of HoBi is indicated in the inset of Fig. 3. Here, we pay more attention to the magnetization behavior in the [100] direction, because it has the potential to lead to a larger positive MCE than in the [110] direction.

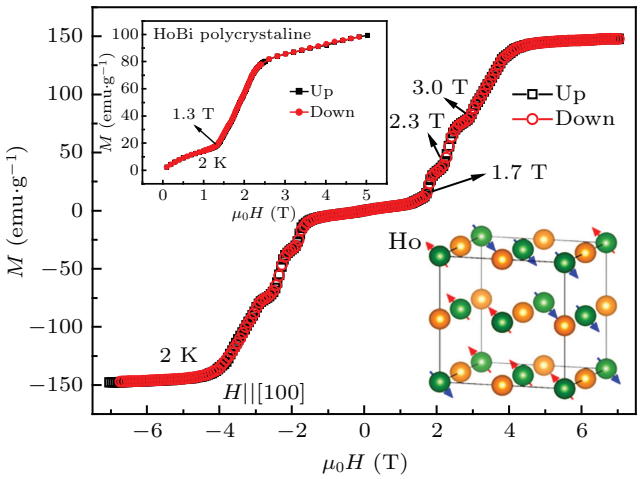


**Fig. 3.** Magnetic hysteresis loops of Hobi at 2 K with $H \parallel [100]$ direction, in a field range from −7 T to 7 T, with upper-left inset showing magnetic hysteresis loops of HoBi polycrystalline at 2 K in a field range from 0 T to 5 T, and bottom-right inset describing magnetic structure of HoBi.

The isothermal magnetization curves for HoBi compounds are measured in applied fields up to 5 T in the vicinity of $T_N$ as indicated in Figs. 4(a) and 4(b). The magnetization of HoBi polycrystalline is lower than the counterpart in the [100] direction under high filed. Below the temperature $T_N$, the magnetization curve of HoBi polycrystalline linearly increases and then suddenly jumps with the increase of magnetic field, indicating the metamagnetic transition from AFM to FM phase. With temperature increasing to $T_N$, the AFM state changes into PM state completely. It is also worth noting that the negative slope of Arrott plot shown in the inset of Fig. 4(a) implies the occurrence of a first-order phase transition.

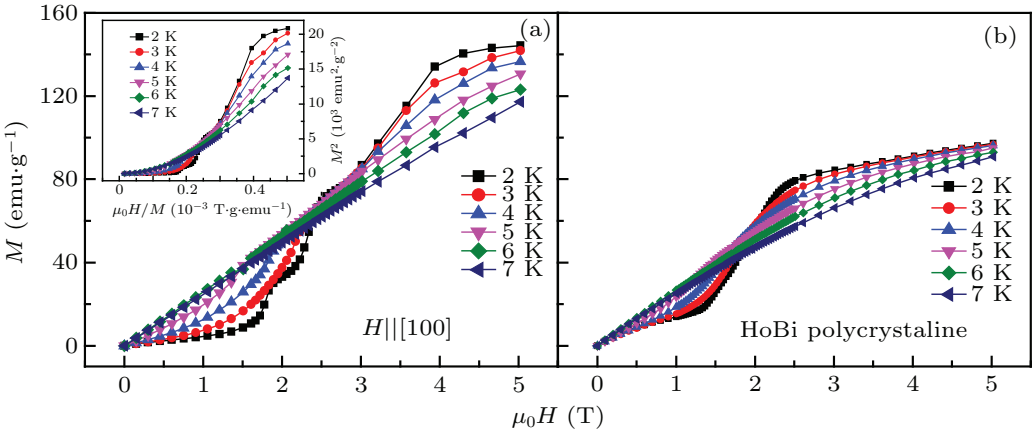


**Fig. 4.** Magnetization isotherms in the vicinity of $T_N$ from 0 T to 5 T field of (a) HoBi single ($H \parallel [100]$) and (b) HoBi polycrystalline.

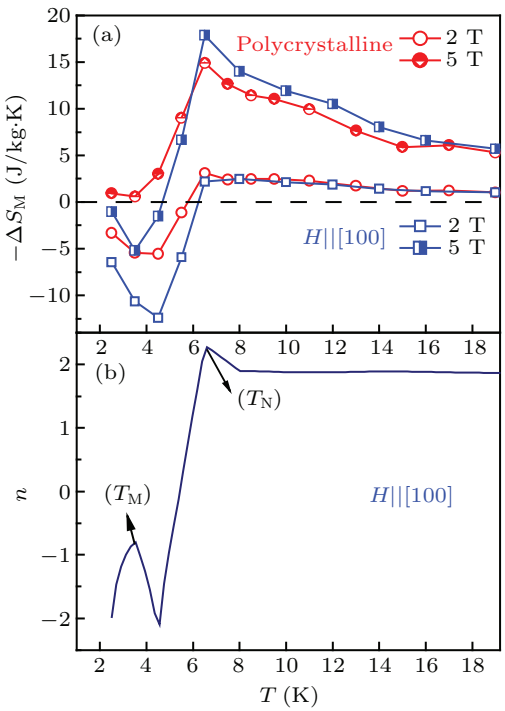


**Fig. 5.** (a) Temperature-dependent $\Delta S_M$ at 0 T–2 T and 0 T–5 T field changes for HoBi single crystal ($H \parallel [100]$) and polycrystalline, respectively, and (b) field and temperature-dependent exponent $n$ for HoBi single crystal.

Magnetic entropy changes in different magnetic fields are calculated from the Maxwell relation $\Delta S_M = \int_0^H \left(\frac{\partial M}{\partial T}\right)_H \mathrm{d}H$ based on the magnetization isotherms. The temperature dependence of $\Delta S_M$ for HoBi compounds under 0 T–2 T and 0 T–5 T field changes are shown in Fig. 5(a). Positive values of $\Delta S_M$ are found at low temperatures. For the HoBi polycrystalline compound, the positive values of $\Delta S_M$ can be found only under a low field change, then disappears with the field change increasing to 5 T, which indicates that the AFM ground state below $T_N$ is relatively weak. The same phenomenon has been found in many Heusler alloys.[19] However, the inverse MCE can be found in HoBi single crystal even in a field change of 5 T due to the strong AFM coupling in the [100] direction. This property is found in a few rare earth based alloys, such as DyNiSi and HoFeSi.[20,21] The maximal positive $\Delta S_M$ reaches 13.1 J/kg·K for a field change −2 T. It is beneficial to practical application, because the magnetic field of 2 T can be provided by a permanent magnet. The maximal negative $\Delta S_M$ reaches 18.0 J/kg·K for the field change 0 T–5 T. From the above analysis, single crystals outperform polycrystals, but polycrystals also show objective magnetocaloric properties. It is also worth mentioning that the $\Delta S_M$ values above $T_N$ broaden asymmetrically towards high temperature under the action of an external field. It may be attributed to the existence of short-range FM interactions above $T_N$.[22] The exponent $n$ dependent on magnetic field change exhibits a maximum value $n > 2$ only for first order phase transitions.[23] As shown in Fig. 5(b), the peak $n$ is higher than 2 at temperatures close to $T_N$, followed by a trend towards $n = 2$ at higher temperatures. It proves exactly that FOMT occurs in HoBi, which is consistent with the previous speculation in this paper. The unusual behavior of $n$ at 4.5 K is due to the magnetic entropy changing from negative to positive, and another peak near $T_t$ corresponds to the maximum value of the inverse MCE.

## 4. Conclusions

In this work, single-phase HoBi single crystal and polycrystalline with cubic NaCl-type structure are successfully prepared. The magnetic properties and MCEs are investigated by magnetic measurements. The HoBi compound with FOMT exhibits good thermomagnetic reversibility and successive large inverse MCE and normal MCE. For the HoBi single crystal, the $\Delta S_M$ peak near $T_t$ reaches 13.1 J/kg·K for a low field change of 2 T and the peak near $T_N$ reaches −18 J/kg·K for a field change of 5 T. These excellent properties are expected to be used to design some special magnetic refrigerators.

## Acknowledgements

Project supported by the Scientific and Technological Innovation Programs of Higher Education Institutions in Shanxi Province, China (Grant No. 2021L304), the Taiyuan University of Science and Technology Scientific Research Initial Funding, China (Grant Nos. 20202022 and 20222002), the Funding for Outstanding Doctoral Research in Jin, China (Grant No. 20212002), the Fund from the State Key Laboratory of Advanced Technology for Materials Synthesis and Processing, Wuhan University of Technology, China (Grant No. 2022-KF-32), and the National Natural Science Foundation of China (Grant No. 51901150).

## References

[1] Gutfleisch O, Willard M A, Brück E, Chen C H, Sancar S G and Liu J P 2011 *Adv. Mater.* **23** 821
[2] Pecharsky V K and Gschneidner K A Jr 1999 *J. Magn. Magn. Mater.* **200** 44
[3] Smith A 2012 *Adv. Energy Mater.* **2** 1288
[4] Gschneider K A Jr, Pecharsky V K and Tsokol A O 2005 *Rep. Prog. Phys.* **68** 1479
[5] Pecharsky V K and Gschneidner K A Jr 1997 *Phys. Rev. Lett.* **78** 4494
[6] Hu F X, Shen B G, Sun J R, Cheng Z H, Rao G H and Zhang X X 2001 *Appl. Phys. Lett.* **78** 3675
[7] Yang S X, Zheng X Q, Yang W Y, Xu J W, Liu J, Xi L, Zhang H, Wang L C, Xu Z Y, Zhang J Y, Wu Y F, Ma X B, Chen D F, Yang J B, Wang S G and Shen B G 2020 *Phys. Rev. B* **102** 134425
[8] Zhang Y, Dong Q Y, Wang L C, Zhang M, Sun J R, Hu F X and Shen B G 2016 *RSC Adv.* **6** 106171
[9] Krenke T, Duman E, Acet M, Wassermann E F, Moya X, Manosa L and Planes A 2005 *Nat. Mater.* **4** 450
[10] Wei L S, Zhang X X, Gan W M, Ding C, Liu C F, Geng L and Yan Y W 2021 *J. Alloys Compd.* **874** 159755
[11] Liu F X, Zhang H, Zhou H, Cong D Y, Huang R J, Wang L C and Long Y 2020 *Sci. China-Phys. Mech. Astron.* **63** 277511
[12] Biswas A, Chandra S, Samanta T, Ghosh B, Datta S, Phan M H, Raychaudhuri A K, Das I and Srikanth H 2013 *Phys. Rev. B* **87** 134420

[13] Liu J, Xu Z Y, Xu J W, Zuo S L, Zhang Y, Liu D, Zheng X Q, Wang L C, Zhao T Y, Hu F X, Sun J R and Shen B G 2020 *J. Magn. Magn. Mater.* **502** 166551
[14] Zhang X X, Zhang B, Yu S Y, Liu Z H, Xu W J, Liu G D, Chen J L, Cao Z X and Wu G H 2007 *Phys. Rev. B* **76** 132403
[15] Guzik A, Talik E and Zajdel P 2020 *Intermetallics* **118** 106686
[16] Fente A, Suderow H, Vieira S, Nemes N M, García-Hernández M, Bud'ko S L and Canfield P C 2013 *Solid State Commun.* **171** 59
[17] Yang H Y, Gaudet J, Aczel A A, Graf D E, Blaha P, Gaulin B D and Fazel Tafti 2018 *Phys. Rev. B* **98** 045136
[18] Alho B P, Ribeiro P O, von Ranke P J, Guillou F, Mudryk Y and Pecharsky V K 2020 *Phys. Rev. B* **102** 134425
[19] Krenke T, Duman E, Acet M, Wassermann E F, Moya X, Manosa L and Planes A 2005 *Nat. Mater.* **4** 450
[20] Zhang B, Zheng X Q, Zhang Y, Zhao X, Xiong J F, Zuo S L, Liu D, Zhao T Y, Hu F X and Shen B G 2018 *AIP Advances* **8** 056423
[21] Zhang H, Sun Y J, Yang L H, Niu E, Wang H S, Hu F X, Sun J R and Shen B G 2014 *J. Appl. Phys.* **115** 063901
[22] Arora P, Chattopadhyay M K, Chandra L S S, Sharma V K and Roy S B 2011 *J. Phys.: Condens. Matter* **23** 056002
[23] Law J Y, Franco V, Moreno-Ramírez L M, Conde A, Karpenkov D Y, Radulov I, Skokov K P and Gutfleisch O 2018 *Nat. Commun.* **9** 2680